

Metal as Insulation REBCO Racetracks Coils: Development, Fabrication, and Cryogenic Testing at CEA Paris-Saclay

Thibault Lecrevisse¹, Emeric Benoist¹, Audren Blondelle, Antomne Caunes¹, Matthias Durochat¹, Clément Genot¹, Gilles Lenoir¹, Bruno Maloeuvre, Amalia Ballarino², and Algirdas Baskys²

Abstract—CEA-Saclay started the development of Metal-as-Insulation racetrack coils in as part of the High Field Magnet (HFM) CERN program. This winding method aims to significantly reduce the amount of High Temperature Superconductor material required to achieve relatively high magnetic induction and associated forces. CEA's objectives are to fabricate and test a small racetrack coil to benchmark numerical models with experimental data. The insulated coil counterpart, operating at lower current densities and targeting high fields, is studied by CERN as part of the HFM program. This paper focuses on the design, fabrication and quench tests at 4.2 K of two specific coils: a single racetrack coil and a double racetrack coil (DRT), each with 140 mm long straight part and 27 mm inner diameter. Both coils achieved very high overall current density (above 2300 A/mm²) and significant peak magnetic field on the conductor (8.5 T and 12.3 T respectively). A central magnetic field above 5 T was reached after a quench at 4.3 T in the DRT.

Index Terms—Metal-as-Insulation, MI racetrack, REBCO racetrack, high field dipole, accelerator magnet, racetrack quench, racetrack fabrication.

I. INTRODUCTION

HIGH Temperature Superconductors (HTS) offer significant potential for very high field dipole. We started the development of insulated HTS REBCO dipole magnets in 2010, by participating in the EUCARD [1] and EUCARD2 [2] programs. CEA Paris-Saclay then chose to apply the Metal-as-Insulation (MI) REBCO windings [3], originally developed in the 32.5 T solenoid insert project NOUGAT [4], to HTS high field dipoles, in order to enhance their design, fabrication and performances.

Received 26 July 2025; revised 24 September 2025; accepted 17 October 2025. Date of publication 3 November 2025; date of current version 17 November 2025. This work was supported in part by CERN High Field Magnet Program through CERN-CEA Collaboration Agreement under Grant HFM/KE5647/TE and in part by French Government for the funding of the winding machine (grant managed by the French National Research Agency through the Future Investment Program (PIA) under Grant PIA3 FASUM ANR-21-ESRE-0027). (Corresponding author: T. Lecrevisse.)

Thibault Lecrevisse, Emeric Benoist, Audren Blondelle, Antomne Caunes, Matthias Durochat, Clément Genot, Gilles Lenoir, and Bruno Maloeuvre are with CEA/IRFU – Paris-Saclay University, 91191 Gif-Sur-Yvette Cedex, France (e-mail: thibault.lecrevisse@cea.fr).

Amalia Ballarino and Algirdas Baskys are with the CERN, European Organization for Nuclear Research, 1217 Geneva, Switzerland.

Color versions of one or more figures in this article are available at <https://doi.org/10.1109/TASC.2025.3628598>.

Digital Object Identifier 10.1109/TASC.2025.3628598

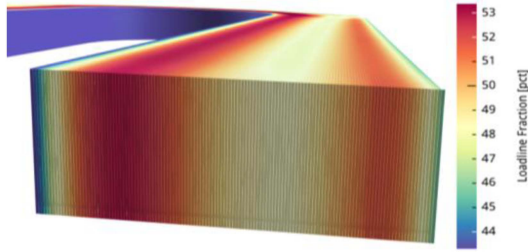
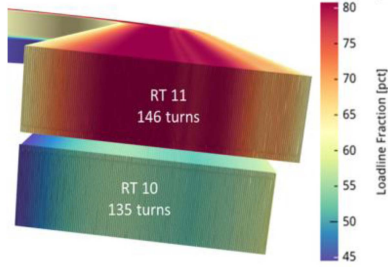
These new developments started in 2023 through the support of a CERN-CEA collaboration as part of High Field Magnet (HFM) CERN program [5]. It is the first step toward a 14 T+ HTS dipole magnet for accelerator machines.

The development strategy involves starting with small, planar coils to validate the numerical design models, then gradually increasing the complexity and associated risks. In this context, we began by modelling and studying the racetrack coil shape. This configuration offers the advantages of planar winding, eliminating the need for hardway bending. The experience on this geometry is therefore easily transferable from the pancake solenoid coils. The MI approach is also well suited for testing models limits because it allows for very compact coils with reduced lengths of REBCO material. Despite the higher complexity of numerical models and a less controlled magnetic field, MI coils present lower degradation risks compared to their insulated counterparts during testing at similar current density. Over the past two years, we have focused on developing the tools for fabricating MI racetrack coils. This includes numerical tools for MI racetrack coil design, as well as tooling and winding procedures. We have also focused on the design of mechanical structures, including the cooling aspects, the stress management, and the assembly of multi-layer racetrack coils. Recently, we fabricated and tested the two mockups including a single short racetrack and a double short racetrack assembly.

We already presented some model and measurement comparisons [6] and, in this paper, we will detail the design and fabrication of the two latest mockups and then describe some experimental measurements at 4.2 K in a liquid helium bath environment. We will focus on the coil quench currents of 1025 A and 915 A, resulting in central magnetic flux densities of 2.9 T and 5.1 T, respectively, for the single and double racetrack coils. Additionally, we will discuss quench protection and the accuracy of the design limits.

II. MOCKUP DESIGN

We prepared three racetrack (RT) coils to be tested at 4.2 K in liquid helium (LHe). The RT9 was tested alone, and the RT10 and RT11 were assembled to form the DRT10-11. All racetracks feature MI windings composed of a co-winding of REBCO Shanghai Superconductor Technology (SST) tape co-wound

Fig. 1. RT9%LL (at 1000 A and 4.2 K) considering $I_{c,min}$.Fig. 2. DRT10-11%LL (915 A and 4.2 K) considering $I_{c,min}$.TABLE I
SHANGHAI SUPERCONDUCTOR TECHNOLOGY REBCO TAPE

Parameter	Unit	RT9	RT10	RT11
SST Tape ID	-	ST2408-1699		ST2408-31
Width (w)	mm		4	
Thickness (t)	μm	75		73
$I_{c,min}$ 77 K, SF	A	263		238
$I_{c,ave}$ 77 K, SF	A	278		256
$I_{c,max}$ 77 K, SF	A	286		265

with a 30 μm thick Durnomag tape from Lamineries Matthey SA.

The RT designs have been adjusted considering the REBCO tape available (dimensions, lengths and performances from the supplier's local I_c measurements at 77 K) and to reach high field and very high current density with a limited amount of tape. The target was to check the design limits and the passive protection of MI RT at very high current density.

Electromagnetic and margin designs are made with GUI-RAT software with the Fleiter-bristow j_c (T, B, α) fit in Appendix A.3 of [7] for SST high field tapes. Using the supplier's minimum critical current of REBCO tape pieces at 77 K ($I_{c,min}$), we adjust the general SST Fleiter-Bristow j_c fit by modifying the thickness of the superconducting layer. We then apply the same fit and thickness at 4.2 K to evaluate the minimum critical current in the racetracks ($I_{c,RT,min}$), accounting for current redistribution across the tape's width. The $I_{c,RT,min}$ are 1890 A and 1125 A for RT9 and DRT10-11 respectively, at 4.2 K, as presented in Figs. 1 and 2, considering the current at 100% of the load-line (%LL, i.e., the maximum operating current set by the superconductor's critical current). The DRT10-11 current should be limited by the RT11 due to the lower performance of the REBCO tape as presented in Table I. The racetrack parameters are presented

TABLE II
RACETRACKS / DOUBLE RACETRACK PARAMETERS

Parameter	Unit	RT9	RT10	RT11	DRT10-11
Tape length	m	53	54	59	113
RT width	mm			27	
Straight part	mm			140	
Average turn thickness	μm	100	96	96	96
Turn number	-	132	135	146	281
Inductance	mH	3.12	3.27	3.79	12.56
$\alpha_{center,min}$ *	mT/A	2.85	2.93	3.10	5.89
$\alpha_{center,max}$ *	mT/A	2.88	2.98	3.14	5.95
$\alpha_{peak\ tape}$ *	mT/A	8.30	8.58	8.88	13.50

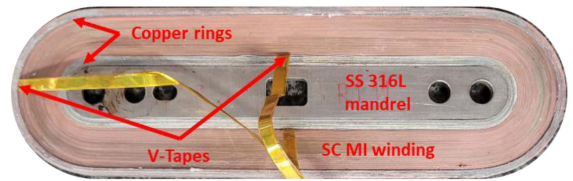


Fig. 3. RT11 picture.

and Table II (calculated parameters from real coils geometry and tapes). The magnetic field-current ratio at the center is denoted as $\alpha_{center,max}$ when considering the soldered turns for the current transfer to the copper rings, and as $\alpha_{center,min}$ when not considering the soldered turns.

III. FABRICATION

The RT winding process utilizes the winding machine available since Summer 2023. The RT fabrication consists of three main phases:

- The fabrication of the inner copper ring which is the racetrack's current lead. This ring is made of 30 turns of 100 μm copper tape tinned with Pb37Sn63 solder. The ring is soldered by heating the whole ring at 210°C.
- The main winding composed of a REBCO tape co-wound with a Durnomag tape. Both tapes are soldered to the copper rings with Pb37Sn63 solder. The superconducting layer facing inward, and soldered to the copper over 80% of a turn to the inner and outer copper ring.
- The fabrication of the outer copper ring similar to the inner copper ring but uses an In48Sn52 alloy to reduce the heating temperature and prevent damage to the previous soldered parts.

The winding stress is constant during the winding process: 110 MPa (REBCO) and 125 MPa (Durnomag) for the RT9 and RT10, and 133 MPa (REBCO) and 150 MPa (Durnomag) for the RT11.

Four voltage taps are included in the windings: one after the soldered turn and after the first (or before the last) turn.

A View of the RT10 including the copper rings is presented in Fig. 3.

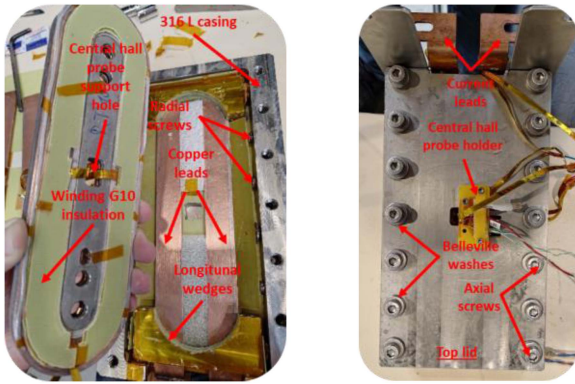


Fig. 4. DRT10-11 during assembly (left) and closed structure before mounting on probe (right).

The Racetracks are then inserted into the test structure, which is designed to handle the mechanical forces at maximal current by constantly maintaining radial compression on the turns (mainly on the straight parts using Belleville washers). This compression is mandatory to keep the passive protection (i.e., self-protection) of MI coils. This structure includes also a Hall probe holder at the center. Current is fed from the power supply through copper busbars (two per side), which are identical for inner and outer rings (insulation between the coil and busbars allows selection of which rings is connected). Images of the assembly process of DRT10-11 and of the final coil casing are presented in Fig. 4.

IV. TESTS RESULTS IN LHE BATH

A. Test Station Configuration

The test station is located at CNRS Néel Institute in Grenoble and consists of a 10 V / 1.2 kA Sorensen Power supply, a cryostat allowing test at LHe temperature, and a probe for the coils handling which includes many twisted wire pairs and 3 kA current leads cooled by cold He vapors.

The signals are recorded with a National Instrument c-DAQ system, which includes NI 9226, NI 9229, NI 9238 and NI 9239 modules for voltages measurements (coils voltages and Hall probe) and temperature measurements (Cernox sensors). Two Hall probes, calibrated up to 20 T at LNCMI (Asensor HE244 and Arepoc HHP-NP), are installed at the magnet center. The tests are controlled using a custom LabView program.

B. Results on Single Racetrack (RT9)

In this section we are presenting the quench sequences related to the RT9 coil (single RT test). The objective is to check the quench current and evaluate the self-protection behavior at very high current density (estimated over 4500 A/mm^2).

The first quench sequence is presented in Fig. 5, following a step-by-step approach. The coil was initially energized at 10 A/s up to 500 A and then at 2 A/s with 100 A steps. The coil quenched at 1025 A (peak current before voltage limitation of $\sim 54\%$ of estimated limit) and reached 2.9 T at center (8.5 T estimated peak field on REBCO tape) at 2560 A/mm^2 in the winding pack. This

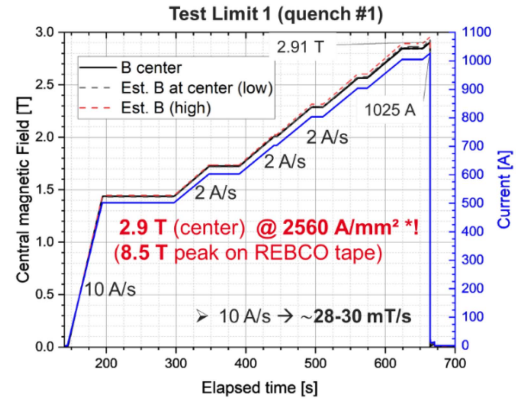


Fig. 5. RT9 quench #1 test at 4.2 K.

*Overall current density.

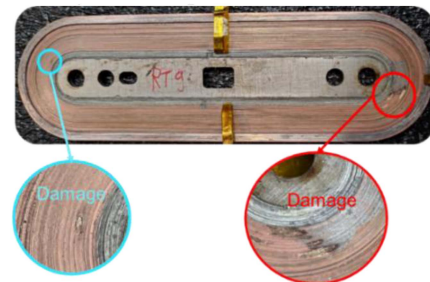


Fig. 6. View of damage in RT9.

value is about 4–5 times the current density of classical low temperature superconducting magnets in accelerator machines [5;8]. The simple protection scheme for this test relies on a power supply voltage limitation at 2.7 V. The dynamic of the quench is similar to the DRT10-11 one (Fig. 7). The coil internal resistance increased from $150 \text{ n}\Omega$ to $69 \text{ m}\Omega$ within 165 ms. With this passive protection, approximately 40 J were injected by the power supply during the quench event and 200 J within the 6 s of voltage limitation (to be compared with the $\sim 1.6 \text{ kJ}$ of stored energy). After this quench, we charged the coil at different ramp rates to evaluate the coil behavior and it quenched at lower currents (770 A, 625 A and 567 A respectively for quenches #2, #3 and #4) indicating some incremental damage to the coil during each quench. The damages are visible in Fig. 6 in curved parts of the racetrack. The turn-to-turn resistance is estimated to exceed $60 \mu\Omega/\text{turn}$ (potentially be even higher), thus we can assume that the coil is still superconducting up to the quench with a total coil resistance of only $\sim 300 \text{ n}\Omega$ at 500 A. This resistance comparison suggests that the damages visible in Fig. 6 only affect a fraction of the tape width.

C. Results on Double Racetrack (DRT10-11)

Following the tests of the RT9, we assembled and tested the DRT10-11 (i.e., RT10 and RT11 are tested together in the structure). Following the same step by step approach as for RT9, we reached a first quench at 828 A (i.e., $\sim 74\%$ of the estimated limit). At this current (corresponding to $j_{\text{overall}} \sim 2150 \text{ A/mm}^2$), the measured central magnetic field was 4.6 T. Compared to the

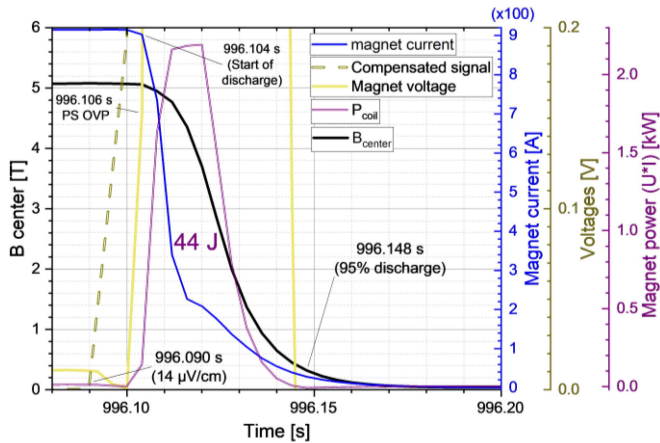


Fig. 7. DRT10-11 Second quench zoom.

RT9 test, the passive protection relied on a power supply Over Voltage Protection (OVP) set at 0.5 V to limit the energy injected by the power supply during and after the quench.

A second quench test was conducted to assess the magnet's condition, maintaining the same step by step approach. This time the coil reached 915 A ($\sim 81\%$ of the estimated current limit). The measured central magnetic field reached ~ 5.1 T (at $j_{\text{overall}} \sim 2380$ A/mm²). The peak magnetic field on REBCO tape is estimated to be ~ 12.3 T (without magnetization effect). The quench details are presented in Fig. 7. The coil voltage increased above 2 V within ~ 20 ms after the detection voltage on compensated signal. Considering the OVP at 0.5 V, we can estimate that ~ 4 J have been injected in the coil and that ~ 41 J have been extracted through the PS protection circuit. This value should be compared to the 5.2 kJ of stored energy in the magnet. If distributed homogeneously within a single racetrack, the temperature would increase by 125 K. If distributed in the two racetracks, peak temperature would increase by 90 K.

A final test was performed at 500 A (to minimize risks to the current leads due to the low remaining LHe level), which showed no significant changes in inductance or resistances for either RT10 and RT11 between the first and the last tests. This statement was confirmed by a visual inspection of the racetracks, which revealed no burnt areas, in contrast to the damage observed in RT9.

V. DISCUSSION

The two tested mockups demonstrated high performances and survived quenches at very high current densities (above 2500 A/mm² for RT9 and above 2300 A/mm² for DRT10-11), despite localized damages in the case of RT9. Very high peak magnetic field (8.5 T and 12.3 T respectively) were achieved at these current densities. The results reaffirm the attractiveness of MI winding technology, which enables mechanically robust coils ($\sim 90\%$ of stainless steel or equivalent in the winding) that are easier to protect at very high current densities compared to insulated coils. The absence of damage in DRT10-11 confirmed the self-protection behavior for low energy magnets (although with a high winding mass energy of ~ 13 kJ/kg). For both

mockup coils, almost all the stored energy was dissipated inside the winding and the OVP helped to reduce the energy dissipation in the coils during and after the quench. The protection behavior still requires further understanding to optimize the protection scheme (potentially combining passive and active protection) and improve the energy extraction outside of the coil if possible. In our case, almost all the stored energy (1.6 kJ for RT9 and 5.2 kJ for DRT10-11) was dissipated within the winding. A numerical transient model is required to evaluate the real hotspot reached. Assuming that the energy is dissipated evenly within the whole winding pack, the peak temperature should have reached about 80 K.

Our design approach, which considers the ultimate limit when the whole tape width is saturated seems wrong for the two tested coils, as it only reached 54% and 81% of the estimated limit for RT9 and DRT10-11, respectively. When considering the local limit (no current redistribution) with respectively $I_{c,\text{min}}$ and $I_{c,\text{max}}$ of Table I for RT9 and DRT10-11, the coils reached 80% and 105% of the calculated limit, respectively. It shows that estimates are highly dependent on the assumptions made, and in case of very high current density coils, the assumption of full current saturation of the tape seems overly optimistic.

Another aspect not included in the models relates to the screening currents and associated mechanical issues at the tape edges (where burnt areas were observed), as presented in ultra-high field NI coils [9], [10]. It could cause local instabilities leading to premature quench in RT9, where the current margins should be higher (compared to RT10-11). In the absence of reliable numerical models for evaluating the screening currents inside the REBCO (model development is ongoing), we can only notice that the very high current density within the REBCO tape (>3660 A/mm² for RT9 and >3450 A/mm² for DRT10-11) represents values never studied in REBCO insulated pancakes but made possible by MI technology. The corresponding current density within the copper exceeds 15 kA/mm². Despite these extreme values, both coils exhibited a stable behavior close to the quench current (30 s above 97% and 99% of quench current for RT9 and DRT10-11 respectively).

This discussion highlights the complexity of anticipating the real coils margins (e.g., whether the minimum I_c is localized in the worst location within the winding) and therefore the necessity to experimentally measure the quench currents on representative mockups or final coils without damaging them.

VI. CONCLUSION

We have developed a good process of fabricating very compact short (140 mm straight part length) MI REBCO coils. The setup allows also to test them up to their limits in standalone at 4.2 K. We succeeded to measure above 5 T at center of one double racetrack coil corresponding to a peak magnetic field on the conductor of 12.3 T at an overall current density above 2300 A/mm². The double racetrack survived to the quench despite an energy density close to 13 kJ/kg inside the winding, thanks to the MI winding coupled with the power supply OVP. This limit is about 20% lower than expected from the model considering the full current saturation in the tape. It shows that

we need to be careful when using our models for designing a coil or a magnet. Indeed, the quench initiation mechanism might lead to a wrong estimation. This is specially the case at very high current density where the quench initiation might be related to a local instability. We succeeded to quench above the theoretical limit when considering the local load-line of the DRT10-11 instead of the load-line with redistribution. If we still need to investigate the possibility of quench induced by a local overstress on the edges of the tapes due to the magnetization, we will continue the experimental measurements to confirm the presented results and improve our model accuracy. We also would like to go on longer racetrack (600 mm of straight part length) in order to prepare the next step which will be a 14 T+ block MI REBCO dipole.

ACKNOWLEDGMENT

The authors express their gratitude to colleagues from CNRS Grenoble for their great help during the 4.2 K tests and in particular A. Badel, J. Vialle and P. Tixador from Néel Institute and X. Chaud and J.-B. Song from LNCMI.

REFERENCES

- [1] M. Durante et al., "Realization and first test results of the EuCARD 5.4-T REBCO dipole magnet," *IEEE Trans. Appl. Supercond.*, vol. 28, no. 3, Apr. 2018, Art. no. 4203805, doi: [10.1109/TASC.2018.2796063](https://doi.org/10.1109/TASC.2018.2796063).
- [2] M. Durante et al., "Manufacturing of the EuCARD2 Roebel-based cos-theta coils at CEA saclay," *IEEE Trans. Appl. Supercond.*, vol. 30, no. 4, Jun. 2020, Art. no. 4602505, doi: [10.1109/TASC.2020.2978788](https://doi.org/10.1109/TASC.2020.2978788).
- [3] T. Lécrovisse et al., "Metal-as-insulation HTS coils," *Supercond. Sci. Technol.*, 2022, vol. 35, Art. no. 074004, doi: [10.1088/1361-6668/ac49a5](https://doi.org/10.1088/1361-6668/ac49a5).
- [4] P. Fazilleau et al., "38 mm diameter cold bore metal-as-insulation HTS insert reached 32.5 T in a background magnetic field generated by resistive magnet," *Cryogenics*, vol. 106, 2020, Art. no. 103053, doi: [10.1016/j.cryogenics.2020.103053](https://doi.org/10.1016/j.cryogenics.2020.103053).
- [5] E. Todesco, "Status and perspectives of high field magnets for particle accelerators," *IEEE Trans. Appl. Supercond.*, vol. 35, no. 5, Aug. 2025, Art. no. 4003914, doi: [10.1109/TASC.2025.3558196](https://doi.org/10.1109/TASC.2025.3558196).
- [6] A. Blondelle et al., "Racetrack-shaped HTS coils with metal-as-insulation: Transient behavior model and experimental validation status," *IEEE Trans. Appl. Supercond.*, vol. 35, no. 5, Aug. 2025, Art. no. 4605007, doi: [10.1109/TASC.2025.3542344](https://doi.org/10.1109/TASC.2025.3542344).
- [7] J. van Nugteren, "High temperature superconductor accelerator magnets." Ph.D. dissertation, Univ. Twente, Enschede, The Netherlands, 2016. [Online]. Available: <https://research.utwente.nl/en/publications/high-temperature-superconductor-accelerator-magnets/>
- [8] E. Rochepault et al., "3D Conceptual design of R2D2, the research racetrack dipole demonstrator," *IEEE Trans. Appl. Supercond.*, vol. 32, no. 6, Sep. 2022, Art. no. 4004605, doi: [10.1109/TASC.2022.3158634](https://doi.org/10.1109/TASC.2022.3158634).
- [9] S. Hahn et al., "45.5-tesla direct-current magnetic field generated with a high-temperature superconducting magnet," *Nature*, vol. 570, pp. 496–499, 2019, doi: [10.1038/s41586-019-1293-1](https://doi.org/10.1038/s41586-019-1293-1).
- [10] J. Park, J. Bang, U. Bong, J. Kim, D. Abraimov, and S. Hahn, "Parametric study on effect of friction and overbanding in screening current stress of LBC magnet," *IEEE Trans. Appl. Supercond.*, vol. 31, no. 5, Aug. 2021, Art. no. 4603205, doi: [10.1109/TASC.2021.3070097](https://doi.org/10.1109/TASC.2021.3070097).